Remote Preparation of Single-Photon "Hybrid" Entangled and Vector-Polarization States

Julio T. Barreiro,[1,2] Tzu-Chieh Wei,[1,3] and Paul G. Kwiat[1]

[1]*Department of Physics, University of Illinois at Urbana-Champaign, Urbana, Illinois 61801-3080, USA*
[2]*Institut für Experimentalphysik, Universität Innsbruck, Technikerstrasse 25, A-6020 Innsbruck, Austria*
[3]*Department of Physics and Astronomy, University of British Columbia, Vancouver, British Columbia, Canada*

Quantum teleportation faces increasingly demanding requirements for transmitting large or even entangled systems. However, knowledge of the state to be transmitted eases its reconstruction, resulting in a protocol known as remote state preparation. A number of experimental demonstrations to date have been restricted to single-qubit systems. We report the remote preparation of two-qubit "hybrid" entangled states, including a family of vector-polarization beams. Our single-photon states are encoded in the photon spin and orbital angular momentum. We reconstruct the states by spin-orbit state tomography and transverse polarization tomography. The high fidelities achieved for the vector-polarization states opens the door to optimal coupling of down-converted photons to other physical systems, such as an atom, as required for scalable quantum networks, or plasmons in photonic nanostructures.

Quantum communication involves the transfer of quantum information, either directly by sending the quantum states or indirectly by using quantum and classical resources. The cost of indirect transfer involves a trade-off between ebits, units of entanglement, and cbits, units of classical communication, which depends on what is known about the state to the sender and receiver. For example, in teleportation [1], an *unknown* quantum state is sent via a quantum channel, consuming 1 ebit, and 2 bits of classical communication. In contrast, if the state is *known* to the sender, the required resources can be reduced to 1 ebit and 1 cbit, in a protocol named remote state preparation (RSP) [2–5]. This variant of teleportation has received much attention lately, given its reduced resource requirements and known optimal schemes and trade-offs [6–8].

In RSP, Alice wishes to prepare a state in Bob's laboratory by relying on the correlations of shared entangled states and classical communication. RSP not only requires fewer resources than teleportation, but also escapes the need for Bell-state analysis (BSA), impossible with linear optics, but enabled by hyperentanglement [9–12]. RSP has been realized for arbitrary one-qubit states with varying efficiencies. The first demonstration was 50% efficient [13], at the price of 1 ebit and 1 cbit, due to the impossibility of a universal NOT operation on arbitrary qubit states. Subsequent demonstrations achieved 100% efficiency in principle, but required as many resources as teleportation (1 ebit, 2 cbits) [14,15]; however, BSA was not necessary.

In this Letter, we show that by working in a larger Hilbert space, RSP can be extended to remotely prepare multiqubit states, including entangled states [16]. We implement this protocol with a cost of 2 ebits, and 2 cbits of forward classical communication (4 cbits for sending completely arbitrary pure states, as shown below). We then extend it to prepare mixed states and a four-parameter family of pure states. The latter includes a remarkable

family of states with nonuniform transverse polarization, so-called vector-polarization states [17]. These states are important for their applications in improved metrology [18], ideal production of plasmons [19], and in principle 100%-efficient coupling to an atom [20].

Specifically, by using hyperentanglement, i.e., systems simultaneously entangled in multiple degrees of freedom [21,22], we remotely prepare single-photon states entangled in their spin and orbital angular momentum (OAM) [12]. Such "hybrid" entanglement [23–27] between the polarization and the spatial mode of a single photon can be easily converted into a spatially separated single-particle state established to be entangled [28]. In our remote entangled-state preparation (RESP) protocol, Alice and Bob share a hyperentangled pair, e.g., a product of Bell states of polarization and spatial modes $\Phi_{\text{spin}}^+ \otimes \Psi_{\text{orbit}}^+ \equiv (|HH\rangle + |VV\rangle)/\sqrt{2} \otimes (|lr\rangle + |rl\rangle)/\sqrt{2}$, where H (V) represents the horizontal (vertical) photon polarization and l (r) represents the paraxial spatial mode (Laguerre-Gauss) carrying $+\hbar$ ($-\hbar$) units of OAM [29]. For operations on individual photons, we rewrite the shared state in the single-photon basis as [12]

$$\Phi_{\text{spin}}^+ \otimes \Psi_{\text{orbit}}^+ = \frac{1}{2}(\phi_A^+ \otimes \psi_B^+ + \phi_A^- \otimes \psi_B^-$$
$$+ \psi_A^+ \otimes \phi_B^+ + \psi_A^- \otimes \phi_B^-), \quad (1)$$

where the single-photon "spin-orbit" states have the Bell-state form: $\phi^\pm \equiv \frac{1}{\sqrt{2}}(|Hl\rangle \pm |Vr\rangle)$, $\psi^\pm \equiv \frac{1}{\sqrt{2}}(|Hr\rangle \pm |Vl\rangle)$. Thus, when Alice measures her photon (A) with a spin-orbit BSA, the state of Bob's photon (B) is projected into one of the four spin-orbit entangled states $\phi_B^\pm$, $\psi_B^\pm$, according to Alice's outcome $\psi_A^\pm$, $\phi_A^\pm$. Alice can remotely prepare Bob's single photon into a desired spin-orbit entangled state by letting him know the correcting unitary transformation in 2 cbits; e.g., to prepare ψ_B^+, Alice tells

Bob to do nothing if her outcome is ϕ_A^+, transform $V \rightarrow -V$ for ϕ_A^-, $H \leftrightarrow V$ for ψ_A^+, or $V \rightarrow -V$ and $H \leftrightarrow V$ for ψ_A^-.

We implemented this RESP protocol using our spin-orbit BSA and tomographically reconstructed the remotely prepared states (Fig. 1; for details on our source and spin-orbit BSA, see [12,30]). The tomographic measurements are similar to those used for hyperentangled states [22], but in this case applied only to Bob's photon. The spin-orbit state tomography consists of polarization tomography, performed by liquid crystals and a polarizing beam splitter (PBS), and spatial-mode tomography, realized by mode-transforming holograms and single-mode fibers. Figures 2(a)–2(d) show the reconstructed density matrices of the four canonical, remotely prepared, spin-orbit Bell states. The high quality of the prepared states is captured in Table I, where we quote their fidelity with the target state, degree of entanglement (tangle), and mixture (linear entropy) [31].

Note that the spin and orbit d.o.f. of Bob's particle become entangled without local interaction; the above protocol thus realizes entanglement swapping. However, instead of swapping the entanglement between two pairs of particles, here the swapping occurs between pairs of degrees of freedom. The high quality of our scheme (measured fidelities $\approx 95\%$), compares favorably to the best reported for entanglement swapping [32].

In order to use the protocol to remotely prepare mixed states, Alice needs to induce decoherence on Bob's photon. One way to achieve this is by entangling the quantum system to yet another of its d.o.f., which is then traced

over. This technique has previously enabled the precise remote preparation of single-qubit mixed states [13]. There, Alice coupled her photon's polarization and frequency d.o.f. followed by a frequency-insensitive measurement, thus preparing Bob's photon in a mixed state. Similarly, for RESP, Alice can couple the OAM and frequency d.o.f. by detuning the spin-orbit BSA interferometer. After a frequency-insensitive measurement, Alice measures spin-orbit mixed states, preparing Bob's photon in a controllable spin-orbit mixed state.

Alternatively, we can trace over Alice's photon spin and/or orbital d.o.f. or a subspace of them. For example, consider the spin-orbit BSA without either half-wave plates (HWPs) or PBSs (see Fig. 1). In this case, instead of the outcomes ϕ_A^+ and ϕ_A^- (ψ_A^+ and ψ_A^-) we only have the outcome ϕ_A (ψ_A). Consequently, when a pair in the state of Eq. (1) is shared and Alice detects a photon in ϕ_A (ψ_A), Bob's photon is prepared in the classically correlated state $\sim |\psi^+\rangle_B\langle\psi^+| + |\psi^-\rangle_B\langle\psi^-| = |Hr\rangle\langle Hr| + |Vl\rangle\langle Vl|$ or $\sim |\phi^+\rangle_B\langle\phi^+| + |\phi^-\rangle_B\langle\phi^-| = |Hl\rangle\langle Hl| + |Vr\rangle\langle Vr|$,   at the cost of 1 cbit. In addition, by acting on Alice's polarization (as discussed below), we can also prepare classically correlated states in other bases. Furthermore, if both
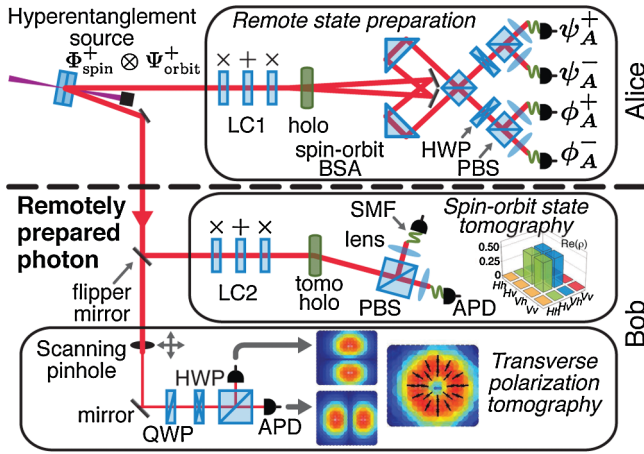

FIG. 1 (color). Experimental setup for the remote preparation of single-photon entangled and vector-polarization states. LC, liquid crystals (LC1 for state preparation, LC2 for polarization tomography) with optic axis perpendicular to the beam and oriented as indicated (+, ×); BSA, Bell-state analyzer; QWP, quarter-wave plate; HWP, half-wave plate; SMF, single-mode fiber; APD, avalanche photodiode; PBS, polarizing beam splitter; holo, forked binary-grating hologram; tomo holo, holograms for spatial-mode tomography [22].
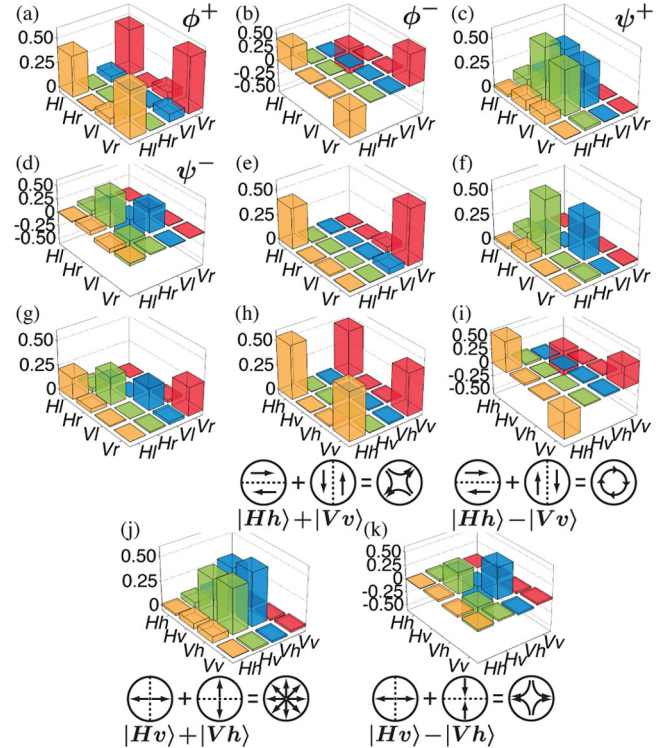

FIG. 2 (color). Experimental density matrices (real parts) of remotely prepared single-photon two-qubit states. (a)–(d) Maximally entangled spin-orbit states, (e),(f) partially mixed states, and (g) completely mixed state. Family of vector-polarization states, (h)–(k), with their ideal polarization profiles shown underneath [spatial-mode component of the density matrix shown in the basis $|h/v\rangle = (|l\rangle \pm |r\rangle)/\sqrt{2}$]. The average magnitude of all imaginary elements, not shown, is 0.02.

TABLE I. Quality parameters of remotely prepared two-qubit states. The first column identifies the states in Fig. 2. Other columns show each prepared-state fidelity (F) with the target state, tangle (T), and linear entropy (S_L). For mixed states we used longer acquisition times, leading to smaller uncertainties. The partially mixed states [2(e) and 2(f)] have an ideal $S_L = 2/3$ and $T = 0$; all others have $S_L = 0$ and $T = 1$, except the completely mixed state 2(g), for which $S_L = 1$ and $T = 0$. All errors are calculated from Monte Carlo simulations of Poissonian counting statistics.

Figure	Target state	F	T	S_L
2(a)	ϕ^+	0.955(2)	0.86(1)	0.06(1)
2(b)	ϕ^-	0.968(2)	0.90(1)	0.06(1)
2(c)	ψ^+	0.938(3)	0.85(2)	0.07(1)
2(d)	ψ^-	0.949(3)	0.85(1)	0.08(1)
2(e)	$(|Hl\rangle\langle Hl| + |Vr\rangle\langle Vr|)/2$	0.967(2)	0.005(2)	0.666(3)
2(f)	$(|Hr\rangle\langle Hr| + |Vl\rangle\langle Vl|)/2$	0.961(3)	0.015(3)	0.658(3)
2(g)	$\frac{1}{4}\mathbb{1}$	0.986(1)	0.000(1)	0.982(1)
2(h)	$(|Hh\rangle + |Vv\rangle)/\sqrt{2}$	0.964(3)	0.88(1)	0.07(1)
2(i)	$(|Hh\rangle - |Vv\rangle)/\sqrt{2}$	0.940(5)	0.82(2)	0.06(1)
2(j)	$(|Hv\rangle + |Vh\rangle)/\sqrt{2}$	0.938(3)	0.82(1)	0.10(1)
2(k)	$(|Hv\rangle - |Vh\rangle)/\sqrt{2}$	0.928(3)	0.81(1)	0.12(1)

spin and OAM of Alice's photon are ignored, Bob's photon is left in a two-qubit completely mixed state (without classical communication). We efficiently prepared such classically correlated and completely mixed states, whose reconstructed density matrices are shown in Figs. 2(e)–2(g).

We can readily remotely prepare a particularly interesting four-parameter family of states by acting on Alice's photon polarization and implementing a modified spin-orbit BSA. Alice and Bob initially share the hyperentangled state $\Phi^+_{\text{pol}} \otimes \Psi^+_{\text{spa}}$. Alice then applies to her photon the polarization unitary operation: $|H\rangle \rightarrow \cos\theta|H\rangle + e^{i\eta}\sin\theta|V\rangle$, $|V\rangle \rightarrow e^{i\phi}(\sin\theta|H\rangle - e^{i\eta}\cos\theta|V\rangle)$; or $e^{i(\eta+\phi)/2}R_z(\eta)R_y(2\theta)R_z(\phi)$, in terms of the Bloch rotation operators, implemented using the LC1 liquid crystals (see Fig. 1). Next, Alice measures her photon with a "rotated" spin-orbit BSA:

$$\phi^+_A(\alpha) \equiv \cos\alpha|Hr\rangle_A + \sin\alpha|Vl\rangle_A,$$
$$\phi^-_A(\alpha) \equiv \sin\alpha|Hr\rangle_A - \cos\alpha|Vl\rangle_A,$$
$$\psi^+_A(\beta) \equiv \cos\beta|Hl\rangle_A + \sin\beta|Vr\rangle_A,$$
$$\psi^-_A(\beta) \equiv \sin\beta|Hl\rangle_A - \cos\beta|Vr\rangle_A.$$

Such a measurement consists of a spin-orbit BSA in which the last polarization measurement is made at the angle α (β) instead of 45° for the $\phi^\pm$ ($\psi^\pm$) output; experimentally, α and β are set with HWPs before the final PBS in Alice's setup, as shown in Fig. 1.

Taking into account the unitary polarization operation and the rotated spin-orbit BSA, we can rewrite the shared state as

$$\Phi^+_{\text{spin}} \otimes \Psi^+_{\text{oam}} \rightarrow \phi^+_A(\alpha) \otimes \phi^+_B(\alpha, \eta, \theta, \phi)$$
$$+ \phi^-_A(\alpha) \otimes \phi^-_B(\alpha, \eta, \theta, \phi)$$
$$+ \psi^+_A(\beta) \otimes \psi^+_B(\beta, \eta, \theta, \phi)$$
$$+ \psi^-_A(\beta) \otimes \psi^-_B(\beta, \eta, \theta, \phi),$$

where Alice's possible outcomes $\phi^\pm_A(\alpha)$ or $\psi^\pm_A(\beta)$ determine Bob's state:

$$\phi^+_B(\alpha, \eta, \theta, \phi) \equiv \cos\alpha|\Xi, r\rangle + e^{i\eta}\sin\alpha|\Xi^\perp, l\rangle,$$
$$\phi^-_B(\alpha, \eta, \theta, \phi) \equiv \sin\alpha|\Xi, r\rangle - e^{i\eta}\cos\alpha|\Xi^\perp, l\rangle,$$
$$\psi^+_B(\beta, \eta, \theta, \phi) \equiv \cos\beta|\Xi, l\rangle + e^{i\eta}\sin\beta|\Xi^\perp, r\rangle,$$
$$\psi^-_B(\beta, \eta, \theta, \phi) \equiv \sin\beta|\Xi, l\rangle - e^{i\eta}\cos\beta|\Xi^\perp, r\rangle,$$

with $|\Xi\rangle \equiv \cos\theta|H\rangle - e^{i\phi}\sin\theta|V\rangle$ and $|\Xi^\perp\rangle \equiv \sin\theta|H\rangle + e^{i\phi}\cos\theta|V\rangle$.

The states in this four-parameter family have the remarkable property that their transverse polarization profiles are not in general uniform [33]. Of outstanding interest is the family of states $\frac{1}{\sqrt{2}}(|Rr\rangle \pm |Ll\rangle)$ and $\frac{1}{\sqrt{2}}(|Rl\rangle \pm |Lr\rangle)$, because of their potentially useful polarization profiles [see Figs. 2(h)–2(k)]. In particular, states with radial polarization profiles [17], such as $|Rr\rangle - |Ll\rangle = |Hv\rangle + |Vh\rangle$, have enabled a focused spot size significantly smaller than possible with linear polarization [18]. Theoretically, such states have also been shown to enable the largest possible longitudinal electric field component in the focal point of a lens [34], leading to optimal coupling to plasmons in subwavelength-diameter holes [19]. Additionally, the radial polarization state is predicted to enable 100% light-atom coupling in free space [20], albeit with a somewhat different radial amplitude distribution.

We remotely prepared a variety of examples from this family of states. Alice's liquid crystals LC1 implement the required polarization unitary, $|H_A\rangle \rightarrow (|H_A\rangle + |V_A\rangle)/\sqrt{2}$, $|V_A\rangle \rightarrow i(|H_A\rangle - |V_A\rangle)/\sqrt{2}$. After measuring Alice's photon with a spin-orbit BSA, we tomographically reconstructed the states of Bob's photon, resulting in the density matrices shown in Figs. 2(h)–2(k).

In order to directly verify the vector profile of the remotely prepared modes, we also implemented a direct transverse polarization tomography. On Bob's beam, at a location with a beam waist size of 1.15(5) mm (measured with the Gaussian component of the down-converted beam), we transversely scanned a 500-μm diameter pinhole in 200-μm steps. At each point in a 16×16 grid, we performed a polarization tomography (6 measurements, 5-sec acquisition time for each). The results of the reconstruction are shown in Fig. 3. We found the expected position of the center of the beam by maximizing the overlap between our measurements and those expected for an ideal beam with our measured waist. As shown in Fig. 3, we achieve a high average fidelity of $\approx 95\%$, over
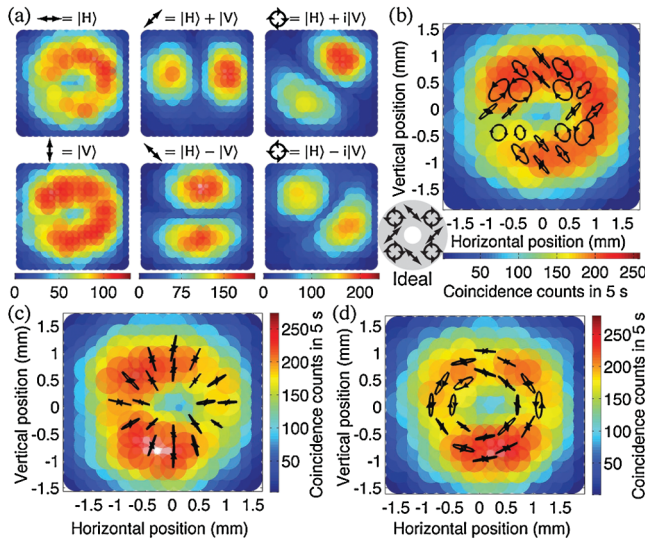
FIG. 3 (color).   Transverse polarization and intensity profiles of remotely prepared vector beams. For a canonical maximally entangled spin-orbit state $\phi^- \equiv \frac{1}{\sqrt{2}}(|Hl\rangle - |Vr\rangle)$, we show (a) the intensity profiles for each polarization projection and (b) the polarization profiles from state tomography at each point; the average fidelity with the target states over all sampled points is $F_{av} = 95(4)\%$. (c) Radial polarization, $F_{av} = 94(4)\%$, and (d) azimuthal polarization, $F_{av} = 95(2)\%$. The polarization ellipses are shown for a subset of all samples, and their size suggests the magnitude of state purity, where pure states have the size of the colored circles (equivalent to the size of the collection pinhole).

all pinhole positions, between the measured and ideal polarizations.

Having discussed the remote preparation of a specific four-parameter family of single-photon states, we can now ask: Can Alice remotely prepare *arbitrary* pure states $\Psi_B(a, b, c, d) = a\phi_B^+ + b\phi_B^- + c\psi_B^+ + d\psi_B^-$ (a–d complex)? The answer is indeed "yes," via the use of positive operator valued measure, as described online [30]. Furthermore, to remotely prepare arbitrary mixed states, Alice can prepare the ensemble of pure states $\{p_i, \psi_i\}$ so that Bob receives $\rho_B = \sum_i p_i |\psi_{B,i}\rangle\langle\psi_i|$.

In summary, we presented the first demonstration of a powerful new technique to remotely prepare a wide variety of single-photon entangled states, using the resource of hyperentangled photon pairs. Some of the states prepared are already known to be optimal for several applications [17], and we anticipate other uses to be revealed by further investigation. A radial polarization state, for example, could enable an optimal plasmon-assisted transmission of entangled photons, remarkably improving earlier demonstrations using entanglement in a single degree of freedom (polarization [35], energy-time [36], and OAM [37]). Furthermore, we have shown how the protocol may be modified to allow the remote preparation of arbitrary two-qubit states. It will be interesting to consider the

generalization to include other degrees of freedom as well, to explore an even richer space of states.

[1] C. H. Bennett *et al.*, Phys. Rev. Lett. **70**, 1895 (1993).
[2] H.-K. Lo, Phys. Rev. A **62**, 012313 (2000).
[3] A. K. Pati, Phys. Rev. A **63**, 014302 (2000).
[4] C. H. Bennett *et al.*, Phys. Rev. Lett. **87**, 077902 (2001).
[5] S. A. Babichev, B. Brezger, and A. I. Lvovsky, Phys. Rev. Lett. **92**, 047903 (2004).
[6] D. W. Berry and B. C. Sanders, Phys. Rev. Lett. **90**, 057901 (2003).
[7] A. Abeyesinghe and P. Hayden, Phys. Rev. A **68**, 062319 (2003).
[8] N. Killoran *et al.*, Phys. Rev. A **81**, 012334 (2010).
[9] P. G. Kwiat and H. Weinfurter, Phys. Rev. A **58**, R2623 (1998).
[10] C. Schuck *et al.*, Phys. Rev. Lett. **96**, 190501 (2006).
[11] M. Barbieri *et al.*, Phys. Rev. A **75**, 042317 (2007).
[12] J. T. Barreiro, T.-C. Wei, and P. G. Kwiat, Nature Phys. **4**, 282 (2008).
[13] N. A. Peters *et al.*, Phys. Rev. Lett. **94**, 150502 (2005).
[14] W. Rosenfeld *et al.*, Phys. Rev. Lett. **98**, 050504 (2007).
[15] W.-T. Liu *et al.*, Phys. Rev. A **76**, 022308 (2007).
[16] J. Liu and Y. Wang, Phys. Lett. A **316**, 159 (2003).
[17] Q. Zhan, Adv. Opt. Photon. **1**, 1 (2009).
[18] R. Dorn, S. Quabis, and G. Leuchs, Phys. Rev. Lett. **91**, 233901 (2003).
[19] H. Kano, S. Mizuguchi, and S. Kawata, J. Opt. Soc. Am. B **15**, 1381 (1998).
[20] M. Sondermann *et al.*, Appl. Phys. B **89**, 489 (2007).
[21] P. G. Kwiat, J. Mod. Opt. **44**, 2173 (1997).
[22] J. T. Barreiro *et al.*, Phys. Rev. Lett. **95**, 260501 (2005).
[23] D. Boschi *et al.*, Phys. Rev. Lett. **80**, 1121 (1998).
[24] Z. Zhao *et al.*, Phys. Rev. Lett. **95**, 030502 (2005).
[25] X.-S. Ma *et al.*, Phys. Rev. A **79**, 042101 (2009).
[26] E. Nagali *et al.*, Phys. Rev. Lett. **103**, 013601 (2009).
[27] L. Neves *et al.*, Phys. Rev. A **80**, 042322 (2009).
[28] S. J. van Enk, Phys. Rev. A **72**, 064306 (2005).
[29] L. Allen, S. M. Barnett, and M. J. Padgett, *Optical Angular Momentum* (IOP, Bristol, 2003).
[30] See supplementary material at http://link.aps.org/supplemental/10.1103/PhysRevLett.105.030407 for details of our hyperentanglement source and a protocol to remotely prepare arbitrary two-qubit states.
[31] A. G. White *et al.*, J. Opt. Soc. Am. B **24**, 172 (2007).
[32] M. Riebe *et al.*, Nature Phys. **4**, 839 (2008).
[33] C. Maurer *et al.*, New J. Phys. **9**, 78 (2007).
[34] H. P. Urbach and S. F. Pereira, Phys. Rev. Lett. **100**, 123904 (2008).
[35] E. Altewischer, M. P. van Exter, and J. P. Woerdman, Nature (London) **418**, 304 (2002).
[36] S. Fasel *et al.*, Phys. Rev. Lett. **94**, 110501 (2005).
[37] X. F. Ren *et al.*, Europhys. Lett. **76**, 753 (2006).